ADVANCED ENERGY & SUSTAINABILITY RESEARCH
Open Access
www.advenergysustres.com

What's Next for Organic Solar Cells? The Frontiers and Challenges

Yasunari Tamai

The power conversion efficiency (PCE) of organic solar cells (OSCs) is improved dramatically in recent years and now approaches >19% for single-junction cells and >20% for tandem cells. Therefore, the practical use of OSCs is becoming a reality. This perspective summarizes the state of the art of OSC characteristics and discusses the challenges that remain in further improving PCE. The short-circuit current density (J_{SC}) of the state-of-the-art OSCs almost approaches 30 mA cm^{-2}. As the internal quantum efficiencies of these devices exceed 90%, for further improvement in J_{SC}, it is necessary to suppress reflection at interfaces and increase the active layer thickness to absorb as many photons as possible. Further suppression of the nonradiative voltage loss is imperative, as there is still large room for improvement compared to inorganic and perovskite counterparts. Hence, increasing the exciton lifetime and photoluminescence quantum yield of nonfullerene acceptors are pivotal to improving the open-circuit voltage of OSCs. The fill factors of the latest OSCs approach 80%; however, because the optimized active layer thickness remains ≈100 nm, further suppression of bimolecular charge recombination is needed. Finally, this perspective discusses to what extent PCE can be improved and what can be done to achieve this.

1. Introduction

Organic solar cells (OSCs) have attracted considerable interest owing to their potential advantages, which include lightweight, thin-film flexibility, color tunability, low toxicity, and low-cost manufacturing. The most significant bottleneck limiting the practical applicability of OSCs has been their poor power conversion efficiency (PCE) (**Figure 1**a), which had lagged far behind those of their inorganic and perovskite counterparts (e.g., PCEs of 26.3% and 26.1% have been reported for silicon and perovskite solar cells).[1] However, the PCE of OSCs has increased spectacularly rapidly in recent years and now approaches 19% for single-junction cells[2] and 20% for tandem cells (Figure 1b).[3] These recent successes have rekindled interest in this research field, and a large number of research articles are being published. This perspective, therefore, briefly summarizes the state of the art of OSC characteristics to highlight the recent advances made with regard to their performance as well as the challenges that remain in realizing further improvements.

The rapid improvements in the PCEs of OSCs in recent years have been largely due to the development of novel nonfullerene acceptors (NFAs).[4] Figure S1 and S2, Supporting Information, show NFAs and donor polymers that are employed in single-junction OSCs with PCEs of over 18%.[2] Most of the acceptors employed in the state-of-the-art OSCs are the so-called Y-series acceptors. In 2019, the prototypical Y-series acceptors, named Y1 and Y2, were synthesized by Yang and coworkers (actually, Y is an abbreviation for Prof. Yang).[5] OSCs consisting of these acceptors paired with a donor polymer PBDB-T exhibited PCEs exceeding 13%. Shortly thereafter, one of the most famous NFAs, named Y6 (also referred to as BTP-4F, 1a in Figure S1, Supporting Information), was synthesized.[6] OSCs consisting of Y6 paired with a fluorinated analogue of PBDB-T, named PM6 (also referred to as PBDB-TF, PBDB-T-F, or PBDB-T-2F, 1d in Figure S2, Supporting Information), exhibited a PCE as high as 15.7%. Therefore, Y6 has recently served as a benchmark NFA, and the latest material design is based thereon, as summarized in Figure S1, Supporting Information. Since then, a very large number of Y6-analogues have been synthesized, many with different lengths or branching positions of the alkyl side chains, or with different terminal halogen (mostly chlorine) atoms. Because we have already accumulated quite a wealth of knowledge just in the past few years, we should make more effective use of informatics, such as machine learning, to develop new acceptors in future research.[7] In contrast, compared to acceptors, there are fewer options for donor polymers (Figure S2, Supporting Information), and PM6 is still used widely in state-of-the-art devices (Table S1 and S2, Supporting

Y. Tamai
Department of Polymer Chemistry
Graduate School of Engineering
Kyoto University
Katsura, Nishikyo, Kyoto 615-8510, Japan
E-mail: tamai@photo.polym.kyoto-u.ac.jp

Y. Tamai
PRESTO Japan Science and Technology Agency (JST)
4-1-8 Honcho Kawaguchi, Saitama 332-0012, Japan

The ORCID identification number(s) for the author(s) of this article can be found under https://doi.org/10.1002/aesr.202200149.

DOI: 10.1002/aesr.202200149

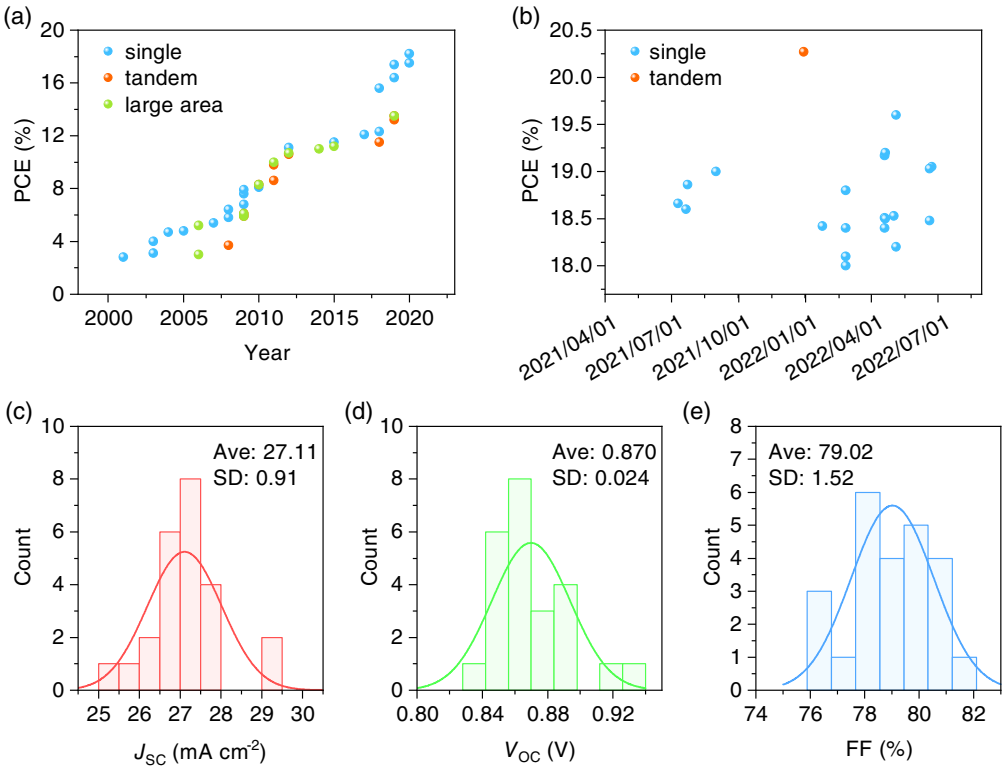

Figure 1. a) Highest certified efficiency of organic solar cells (OSCs) during various periods (until 2020) provided by NREL (https://www.nrel.gov/pv/cell-efficiency.html, last access: October 2022). b) Efficiencies of the state-of-the-art OSCs that exhibit power conversion efficiency (PCE) of over 18% plotted against the date available online.[2b–o] c–e) Histograms of: c) short-circuit current density J_{SC}, d) open-circuit voltage V_{OC}, and e) fill factor (FF) of the state-of-the-art OSCs.[2] The solid line in each panel represents the normal distribution function. Ave and SD in each panel represent average and standard deviation, respectively.

Information). This implies that the development of donor polymers suitable for Y-series acceptors is still in the exploratory phase. Therefore, more effort should be devoted to the development of donor polymers suitable for Y-series acceptors.

Figure 1c–e shows histograms of three representative device parameters, viz., short-circuit current density (J_{SC}), open-circuit voltage (V_{OC}), and fill factor (FF), for the state-of-the-art OSCs.[2] All the parameters exhibited a narrow distribution at a high level. In other words, all the devices showed similar performances and there was no device that exhibited sharp and unique characteristics, implying that there are several common challenges that need to be overcome to improve device performance. Therefore, each parameter is discussed in detail in the following sections.

2. Short-Circuit Current Density

Currently, state-of-the-art OSCs exhibit external quantum efficiencies (EQEs) of over 80% and sometimes reach 90% (albeit only in a limited wavelength region), leading to J_{SC} of 27 mA cm^{-2}, on average (Figure 1c). Although this is already sufficiently high, here, we discuss strategies to improve EQE and J_{SC} further. **Figure 2**a shows the maximum achievable J_{SC} plotted against the optical bandgap E_g (red line) as well as the reported J_{SC}s of the state-of-the-art OSCs (circles).[2] Here, to calculate the maximum achievable J_{SC}, an ideal rectangular EQE spectrum with EQEs of 100% and 0% above and below E_g, respectively, was assumed (i.e., the Shockley–Queisser (SQ) limit was assumed).[8] Figure 2b shows a histogram of the relative error between the ideal and actual J_{SC}s, defined as $(J_{SC}{}^{SQ}-J_{SC})/J_{SC}$, to highlight the extent to which J_{SC} can be improved. As can be seen from the figure, ≈20% of the incident photons with energies greater than E_g are not converted into photocurrent.

How can we reduce this error? EQE of OSCs is a product of the quantum yields (QYs) of the fundamental photophysical processes undergoing in the active layer.[9] When an OSC absorbs the irradiated photons, singlet excitons are generated in either the donor or acceptor domain, which then diffuse randomly and reach the donor:acceptor interface. At the donor:acceptor interface, the excitons separate into charge transfer (CT) states, which are bound electron–hole states trapped at the interface. If the electrons and holes that constitute the CT states dissociate into free carriers, they can be collected at the respective electrodes as photocurrent. Therefore, EQE can be expressed as

$$\mathrm{EQE} = \eta_{abs} \times \eta_{ED} \times \eta_{CT} \times \eta_{CD} \times \eta_{CC} = \eta_{abs} \times \mathrm{IQE} \quad (1)$$

where η_{abs}, η_{ED}, η_{CT}, η_{CD}, and η_{CC} are the QYs of photon absorption, exciton diffusion to the donor:acceptor interface, charge transfer to form a CT state, dissociation of the CT state into free charge carriers, and charge collection at the respective electrodes, respectively. IQE represents the internal quantum efficiency.

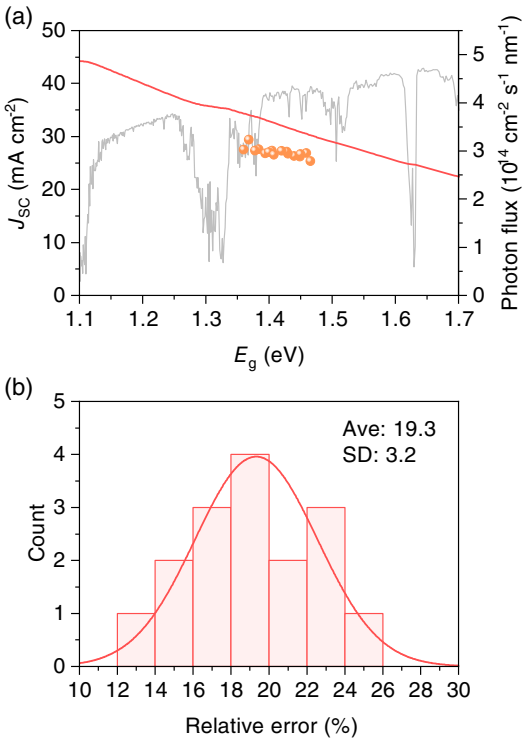

Figure 2. a) J_{SC} of the ideal solar cell, wherein external quantum efficiency (EQE) is 100% and 0% above and below E_g (red line) as well as reported J_{SC}s of the state-of-the-art OSCs (circles).[2] This figure (circles) does not contain data for which E_g was not explicitly mentioned in the literature. This figure (circles) also includes some error in the horizontal direction due to the different methods employed for determining E_g in the literature. The grey line represents the photon flux of the solar spectrum (AM1.5 G) provided by NREL (right axis). b) Histogram of relative error, defined as $(J_{SC}{}^{SQ} - J_{SC})/J_{SC}$, for the state-of-the-art OSCs. The solid line represents the normal distribution function. Ave and SD represent average and standard deviation, respectively.

Previous studies showed that the IQE of the state-of-the-art OSCs exceeded 90% in the broad spectral range of 400 to 900 nm,[2l,2m] meaning that η_{ED}, η_{CT}, η_{CD}, and η_{CC} are ≈98%, on average. For instance, the light-intensity dependence of J_{SC} follows a power-law relation $J_{SC} \propto I^m$, where I is the light intensity, with m close to unity, indicating that bimolecular recombination loss is negligible, at least at short-circuit condition;[2c–f,2h–k] hence, η_{CC} approaches unity. Negligible geminate recombination loss has also been reported for PM6:Y6 blends;[10] thereby, η_{CD} of the state-of-the-art OSCs should be very close to unity as well. Photoluminescence (PL) quenching yields with close to unity have also been reported,[10] meaning that $\eta_{ED} \times \eta_{CT}$ is also close to unity.

Therefore, the largest loss process with respect to EQE involves photon absorption (η_{abs}). A trivial but non-negligible loss source is the reflection of the incident light at interfaces. For instance, ≈4% of the incident photons are reflected at the air/glass interface (assuming that the photons are irradiated perpendicularly to the interface); thereby, η_{abs} will never approach unity unless the reflection at interfaces is suppressed. A more essential challenge is the insufficiency of active layer thickness, which is typically limited to as thin as 100 nm. When the active layer thickness is only 100 nm, η_{abs} in the wavelength range with a low absorption coefficient is significantly lower than unity, even if the absorbance near the absorption maximum is sufficiently high. Therefore, increasing the active layer thickness is necessary to increase η_{abs} and hence EQE/J_{SC}, but this is easier said than done. Increasing the active layer thickness usually degrades the PCE, especially FF, because charge carriers must travel farther in the thicker active layer, resulting in a trade-off between J_{SC} and FF. It should be emphasized that just increasing the charge mobility will not overcome this challenge, as this will also lead to faster bimolecular charge recombination. Therefore, further suppressing bimolecular charge recombination is the top priority for increasing J_{SC}. To this end, increasing the domain size and crystallinity of materials would be key for future research, as will be discussed later again.

Another option to realize substantial improvement in J_{SC} and PCE is the utilization of singlet fission (SF)[11] and triplet–triplet annihilation (TTA).[12] In particular, TTA-upconversion (TTA-UC) is considered to be compatible with solar cell applications because TTA-UC devices can be simply attached to the back side of a solar cell and easily integrated into solar cell technologies. TTA-UC is a photophysical reaction that converts lower-energy photons into higher-energy photons; hence, TTA-UC can beat the energy loss due to transparency in the wavelength range below E_g. A previous study predicted that a PCE of over 30% is expected for TTA-UC-mediated OSCs, even if EQE remains at 85%.[9] Challenges for TTA-UC include the narrow absorption bandwidth of typical triplet sensitizers used in TTA-UC devices and the low efficiencies of TTA-UC in the solid state. The external quantum efficiency (EQE) of TTA-UC (EQE_{UC}) for state-of-the-art solid-state TTA-UC devices remains as low as 2.3% (out of a theoretical maximum of 50%).[13] While previous studies on TTA-UC have focused on increasing the internal quantum efficiency, we must now focus on improving EQE_{UC} as it is more important for the practical application of TTA-UC in solar cell technology.

3. Open-Circuit Voltage

V_{OC} can be divided into two parts

$$V_{OC} = V_{OC}^{rad} - \Delta V_{nr} \tag{2}$$

where $V_{OC}{}^{rad}$ is the radiative limit of V_{OC}, wherein charge recombination is always accompanied by photon emission, and ΔV_{nr} is the nonradiative voltage loss when the QY of radiative charge recombination is lower than unity (**Figure 3**). When E_g is 1.4 eV, which corresponds to E_g of the Y-series acceptors (Figure 2a), $V_{OC}{}^{rad}$ at 300 K can be expressed as

$$V_{OC}^{rad} \approx \frac{E_g}{q} - 0.27 - \Delta V_r \tag{3}$$

where q is the elementary charge, and the term −0.27 originates from the voltage loss due to unavoidable radiative charge recombination as per the detailed balance theory within the SQ framework.[8,14] In contrast, ΔV_r is the nonideal extra radiative voltage loss associated with the photocurrent response in the region below E_g (orange and green shaded regions in

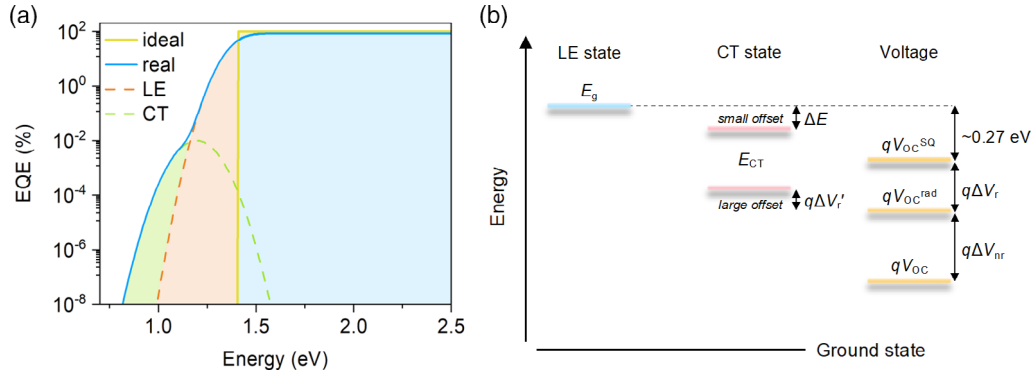

Figure 3. a) Schematic EQE spectra for the ideal solar cell in the SQ framework (yellow line) and realistic OSC (blue line). Here, E_g was set to 1.4 eV. The EQE spectrum for the ideal cell is a step function with EQEs of 100% and 0% above and below E_g. When ΔE is large, the EQE spectrum for the real OSC exhibits a shoulder at lower energies due to charge transfer (CT) absorption (green broken line), which is buried under the local excited (LE) part (orange broken line) when ΔE is small. b) Energy diagram for voltage loss. V_{OC}^{SQ} is the maximum achievable V_{OC} for the ideal cell, which is a function of E_g and temperature and is approximately 0.27 V lower than E_g/q when E_g is 1.4 eV. The imperfection in EQE of the real OSC above E_g region (corresponding to the yellow shaded region in panel (a)) causes a voltage loss; however, this is usually negligibly small compared to other losses as it is proportional to the logarithm of J_{SC}/J_{SC}^{SQ}, as can be inferred from the fact that the yellow shaded region is barely visible in panel (a). CT absorption contributes substantially to ΔV_r when ΔE is large (green-shaded region). In contrast, ΔV_r is governed by the smeared-out absorption edge of nonfullerene acceptors (NFAs) when ΔE is small as the CT part is buried under the LE part (orange-shaded region). Therefore, V_{OC}^{rad} will be maximized by reducing the orange-shaded region by decreasing the degree of the material's disorder. Note that the voltage loss is sometimes discussed with reference to E_{CT}, where the definition of the extra radiative voltage loss (marked as $\Delta V_r'$ in the figure) is different from ΔV_r.

Figure 3a).[15] As the blackbody emission scales exponentially with decreasing energy, the weak shoulder in the EQE spectrum at lower energies due to CT absorption (green line) contributes substantially to ΔV_r when the energy difference ΔE between the local excited (LE) and CT states is large. Because a ΔE of more than 0.3 eV was will, in principle, result charge separation, ΔV_r due to CT absorption is large for prototypical fullerene-based OSCs. One of the most significant recent advances in OSCs is that the latest NFA-based OSCs can generate free charge carriers without the aid of large ΔE, although the mechanism of efficient charge separation without an energy offset remains a subject of continuing debate.[9] Therefore, ΔV_r due to CT absorption is negligible for state-of-the-art OSCs and ΔV_r is governed by the smeared-out absorption edge of NFAs (orange line). This means that V_{OC}^{rad} will be maximized by reducing the degree of the material's disorder. As the Urbach energies of the state-of-the-art OSCs are typically slightly lower than the thermal energy at room temperature (<25 meV),[2i,2k,2m] ΔV_rs of the state-of-the-art OSCs are far less than 0.1 V; hence, there is not much room to increase V_{OC}^{rad}. It should be emphasized that a further reduction in the Urbach energy of OSCs is essential for efficient exciton and charge transport.

In contrast, there is still significant scope to reduce ΔV_{nr}, which is given as

$$\Delta V_{nr} = \frac{k_B T}{q} \ln(EQE_{EL}^{-1}) \quad (4)$$

where k_B is Boltzmann's constant, T is the absolute temperature, and EQE_{EL} is the external quantum efficiency of the electroluminescence (EL) from an OSC device under a forward applied bias. According to Equation (4), one order decrease in EQE_{EL} results in approximately 0.06 V increase in ΔV_{nr}. As EQE_{EL}s of OSCs are significantly lower than those of their inorganic and perovskite counterparts owing to the very low PLQY of the CT states, OSCs exhibit considerably larger ΔV_{nr}. For instance, EQE_{EL}s of prototypical fullerene-based OSCs were typically on the order of 10^{-6}–10^{-8}, which corresponds to ΔV_{nr}s of around 0.4 V.[15,16] In contrast, EQE_{EL}s exceeding 10^{-2} have been reported for silicon solar cells and even $>10^{-1}$ for GaAs and perovskite solar cells.[1]

The importance of reducing ΔE to reduce not only ΔV_r but also ΔV_{nr} has recently been highlighted,[15,17] and has played a considerable role in the recent improvements in V_{OC} and PCE. The radiative decay rate of OSCs increased dramatically with decreasing ΔE, leading to suppression of ΔV_{nr}. **Figure 4** shows a histogram of ΔV_{nr} of the state-of-the-art OSCs.[2] Interestingly, ΔV_{nr} exhibits a very narrow distribution around 0.21 V, which corresponds to an EQE_{EL} of $\approx 3 \times 10^{-4}$ (here, T

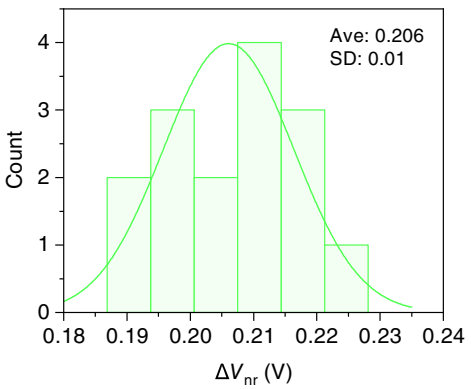

Figure 4. Histogram of ΔV_{nr} for the state-of-the-art OSCs.[2] This figure does not contain data for which ΔV_{nr} was not explicitly mentioned in the literature. The solid line represents the normal distribution function. Ave and SD represent average and standard deviation, respectively.

was assumed to be 300 K). This value is more than two orders of magnitude larger than those of fullerene-based OSCs; however, still lags far behind those of inorganic and perovskite solar cells. Therefore, the next goal should be to reduce ΔV_{nr} down to 0.18 V, which corresponds to an EQE_{EL} of 10^{-3}. Emphatically, while OSCs with ΔV_{nr} of less than 0.18 V have been reported previously many times, what is important here is to achieve a low ΔV_{nr} while maintaining a high EQE and J_{SC}. To the best of my knowledge, there have been no reports of an OSC that simultaneously exhibits an EQE approaching 90% and a ΔV_{nr} lower than 0.18 V. This is because of a decrease in the charge separation efficiency when ΔE becomes too small, implying that a trade-off between the current and voltage still exists even for the latest OSCs.

Then, how can we achieve an EQE_{EL} of 10^{-3} while maintaining a high EQE/J_{SC}? EQE_{EL} can be expressed as

$$EQE_{EL} = \gamma \times \chi \times \Phi_{PL} \times \eta_{out} \quad (5)$$

where γ, χ, Φ_{PL}, and η_{out} are the charge balance factor (often considered to be unity), fraction of emissive states generated after charge recombination (CT states with a spin character of 1 or singlet excitons re-populated through back charge transfer from the CT states), PLQY of the emissive state, and photon out-coupling efficiency, respectively. When γ, χ, and η_{out} are assumed to be 1, 0.25 (considering simple spin statistics), and 0.2, respectively, a Φ_{PL} of 0.02 is necessary to attain an EQE_{EL} of 10^{-3}. This value is comparable to those of pristine donor and acceptor films.

It is quite difficult to determine whether the LE or CT state dominates EL emissions due to the small ΔE of the latest OSCs. Therefore, we consider both patterns here. If CT states dominate the EL emission, the CT states must have a PLQY of 0.02. When the nonradiative decay rate constant k_{nr} of the CT state is assumed to be $10^9\ s^{-1}$, which is typical for OSCs,[15,18] the radiative decay rate constant k_r should be $2 \times 10^7\ s^{-1}$. This is comparable to those of thermally activated delayed fluorescence (TADF) emitters in the field of organic light-emitting diodes (OLEDs).[19] Consequently, this may not be an entirely impossible value, as the central concept of TADF emitters and CT states in OSCs—which involves spatial separation of the highest occupied molecular orbital (HOMO) and lowest unoccupied molecular orbital (LUMO)—remains the same. However, the spatial overlap between the HOMO and LUMO of the CT states in OSCs is typically considerably smaller than those of TADF emitters, resulting in significantly smaller k_r of the former. Therefore, more localization of the HOMO and LUMO at the donor:acceptor interface to increase overlap integral between them may be required to increase k_r. In contrast, the localization of HOMO/LUMO will also result in a concomitant decrease in charge separation efficiency as the delocalization of charge wave functions plays a key role in efficient charge separation,[18,20] and thus is not a viable option. Ideally, Φ_{PL} should be increased by reducing k_{nr} of CT states. Previous studies pointed out that delocalization of the CT state wave function may be pivotal for reducing k_{nr}, and hence, potentially increasing Φ_{PL}.[18]

In contrast, if the LE states re-populated via back charge transfer from CT states dominates the EL emission, Φ_{PL} depends on ΔE as ΔE determines the balance between the populations of LE and CT states. If we assume the PLQY of the LE states (i.e., PLQY of pristine NFA films) to be 0.05,[2b,2m] then the fraction of the LE states re-populated from the CT states must be as high as 40%. Assuming for simplicity that the Boltzmann distribution holds between the CT and LE states, the ratio between the population N of the CT and LE states N_{LE}/N_{CT} can be given as $N_{LE}/N_{CT} = \exp(-\Delta E/k_B T)$, meaning that a low ΔE of $\approx$10 meV is required to attain $N_{LE}/N_{CT} = 40/60$. Such a too small ΔE may simultaneously reduce charge separation efficiency. This is the reason why no OSC exists that simultaneously exhibits EQE approaching 90% and ΔV_{nr} below 0.18 V. So, what should we do? As the fraction of the LE states required to achieve a Φ_{PL} of 0.02 decreases upon increasing the intrinsic PLQY of NFAs, increasing PLQY (i.e., decreasing k_{nr} of the LE states) is pivotal for achieving an EQE_{EL} of 10^{-3}. For instance, the required ΔE increases up to $\approx$50 meV if the PLQY of NFAs is tripled (PLQY of 0.15). Because it is known that a ΔE of 50 meV is sufficient for efficient charge separation, although it depends on the material used,[21] this appears to be a rather realistic estimate.

Another option for increasing EQE_{EL} is to increase χ through the proper spin management of the charge recombination process, which is a core for realizing efficient OLEDs. χ is as low as 0.25 when simple spin statistics are assumed, wherein bimolecular charge recombination produces singlet and triplet CT states with a ratio of 1:3. Moreover, recent studies have pointed out that χ is as low as 0.1 for PM6:Y6 blends owing to the fast back charge transfer from the triplet CT to Y6 triplets.[22] This means that if we can shut the Y6 triplet formation out, EQE_{EL} of the PM6:Y6 device will improve by an order of magnitude. The origin of the fast back charge transfer in PM6:Y6 blends is most probably due to the relatively small energy difference between CT and Y6 triplets.[23] According to the Marcus theory in the normal region,[24] the rate of the back charge transfer decreases with decreasing the CT–triplet energy difference; thereby, further reducing the CT–triplet energy difference will lead to an increase in EQE_{EL}. To this end, reducing the singlet–triplet energy difference of NFAs is essential. Because near-zero or even negative singlet–triplet energy differences have recently been realized in the OLED community,[19,25] if the energy level of the local triplet energy of NFAs can be raised above the CT state energy while maintaining a small ΔE, χ will increase.

4. Fill Factor

The author surmises that the study on FF somewhat lags behind those of J_{SC} and V_{OC}, although FF of state-of-the-art OSCs has gradually increased. FF of the benchmark PM6:Y6 blend in Yuan's report was 74.8%[6] and now FFs of the state-of-the-art OSCs approach 79.02 ± 1.52% (Figure 1e); thereby, OSCs have caught up with other types of solar cells (**Figure 5**). However, there is still large scope to improve FF further. The solid line in Figure 5 represents the well-known empirical relationship between FF and V_{OC}.[26] Although whether or not this empirical relation is valid for OSCs needs to be examined carefully, this is given as

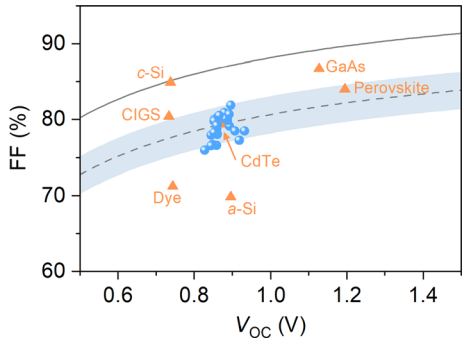

Figure 5. FFs of the state-of-the-art OSCs (circles) as well as certified FFs for other types of solar cells (triangles) obtained from ref.[1] plotted against V_{OC}. The solid line represents the empirical relationship between FF and V_{OC} (Equation (6) with n_{id} and T to be 1 and 300 K, respectively). The broken line and shaded area represent $FF_0 - (0.075 \pm 0.025)$.

$$FF_0 = \frac{\tilde{v}_{OC} - \ln(\tilde{v}_{OC} + 0.72)}{\tilde{v}_{OC} + 1} \tag{6}$$

with

$$\tilde{v}_{OC} = \frac{qV_{OC}}{n_{id}k_BT} \tag{7}$$

FFs of the state-of-the-art OSCs are far below FF_0 (FF_0 is 86.9% when V_{OC} is 0.87 V, which is the average value for the state-of-the-art OSCs (Figure 1d)) and those of high-efficient inorganic solar cells, where FFs of over 85% have been reported.[1] Rather, they follow $FF_0 - (0.075 \pm 0.025)$, as shown in Figure 5 (broken line and shaded area), indicating that there remains scope for improvement in FF by ≈10%.

It should be emphasized that inorganic and perovskite solar cells exhibited such a high FF with active layer thicknesses of more than 500 nm, which is in sharp contrast to OSCs, wherein an active layer thickness of approximately 100 nm is required to maintain a high FF. One of the reasons it is difficult to achieve a high FF with a thick active layer in OSCs may be attributable to the bulk heterojunction (BHJ) architecture of the active layer, wherein the donor and acceptor materials form a bicontinuous interpenetrating network structure. Historically, PCEs of OSCs were dramatically improved by converting the planar heterojunction (PHJ) into the BHJ structure,[27] as it resulted in a larger interfacial area available for charge separation. However, the BHJ structure is detrimental to efficient charge collection because a charge carrier easily encounters an opposite charge in the active layer, resulting in severe bimolecular recombination loss. Recently, attempts have been made to move away from the BHJ structure, leading to an improvement in FF. More specifically, there have been attempts to make a clear phase separation by increasing the domain size or increasing the crystallinity of materials. For instance, sequential deposition (also referred to as layer-by-layer deposition) results in an improvement in FF.[2g,2h,2o] It has been a common belief that increasing the domain size lowers J_{SC} because excitons cannot reach the donor:acceptor interface;[9,28] however, the photophysical background that can help overcome this trade-off is the increase in the exciton diffusion length. The exciton diffusion lengths for prototypical donor polymers are 5–10 nm.[9,28] In contrast, diffusion lengths of more than 20 nm have recently been reported for NFAs owing to their rigid molecular structures,[9,23] which enables increasing the domain size of the donor and acceptor, while ensuring efficient exciton harvesting to the donor:acceptor interface. As an ultimate goal, it would be possible to further improve FF by considering the PHJ structure with further increasing the exciton diffusion length.

On another front for improving FF, reducing ΔV_{nr} would be crucial as FF is a function of V_{OC}.[26] A high V_{OC} will, in principle, result in a high FF; the SQ limit of FF is 89.3% (when E_g is 1.4 eV). As there remains significant scope to improve V_{OC} of OSCs, as mentioned above, FF can be improved by suppressing ΔV_{nr}.

5. Summary and Outlook

In this perspective, the author briefly summarizes the frontiers and challenges for OSCs. The state-of-the-art OSCs exhibit high EQE and J_{SC}; however, there is still scope for further improvement in EQE and J_{SC}. A simple approach to realizing this goal is through light management to suppress the reflection of the incident photons at interfaces. Another option is to utilize TTA-UC to convert the unabsorbed photons with energies lower than E_g into high-energy photons. However, as J_{SC}s of state-of-the-art OSCs are already sufficiently high, in future research, it may be more important to keep J_{SC} high while attempting to improve V_{OC} and FF because of the trade-off between J_{SC} and V_{OC}/FF.

The voltage loss of OSCs is still significantly larger than those of inorganic and perovskite counterparts due to the larger ΔV_{nr} of the former. To reduce ΔV_{nr}, it is essential to reduce ΔE. However, this inevitably leads to slow charge transfer at donor:acceptor interfaces, resulting in decreases in EQE and J_{SC}. To increase the charge separation efficiency with near-zero driving energy, increasing the exciton lifetime is of particular importance for charge transfer to kinetically outcompete deactivation to the ground state.[29] Increasing the PLQY of NFAs and decreasing the energy difference between the singlet and triplet excited states of NFAs are also essential for reducing ΔV_{nr}.

Although FFs of the latest OSCs approach 80%, the optimized active layer thickness remains approximately 100 nm. The key to improving FF or maintaining a high FF with thick active layers is to not consider the BHJ structure as it likely accelerates bimolecular recombination. I believe this is by no means impossible because an exciton diffusion length of more than 200 nm has recently been reported for well-ordered polymer nanofibers.[30]

Finally, the author estimates to what extent the PCE of OSCs can be improved. **Figure 6** shows the estimated PCE as a function of E_g and ΔV_{nr}. Here, J_{SC} is set to $J_{SC}^{SQ} \times 0.85$, assuming approximately 5% improvement in J_{SC} (for instance, the loss due to reflection can be suppressed), whereas FF is set to FF_0–0.06, which has already been achieved for some OSCs. V_{OC} was calculated with Equation (3) with a fixed ΔV_r of 0.08 V and ΔV_{nr} as a variable. As can be seen in the figure, if only all the device parameters (J_{SC}, V_{OC}, and FF) could be improved only slightly, or if only the best values in each column in Table S2,

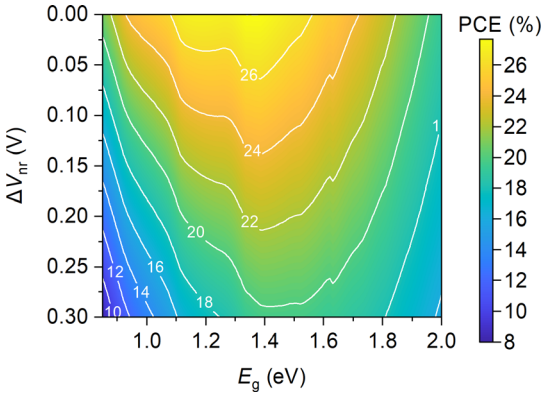

Figure 6. Estimated power conversion efficiency (PCE) as a function of E_g and ΔV_{nr}. Here, J_{SC} is set to $J_{SC}^{SQ} \times 0.85$, and FF is set to $FF_0 - 0.06$. V_{OC} was calculated with Equation (3) with a fixed ΔV_r of 0.08 V and ΔV_{nr} as a variable.

Supporting Information could be combined, a PCE of more than 22% can be expected.

Besides improving PCE, increasing long-term device stability and reducing manufacturing cost are also important for commercialization.[31] Recent studies have shown that a relatively high initial PCE of 17.2% with an extrapolated T_{80} lifetime of 20 500 h (≈2.3 years) can be achieved by all-polymer solar cells.[32] An extrapolated T_{80} lifetime approaching 10 years has also been reported for polymer:NFA-based OSCs, while the initial PCE was ≈8%.[33] However, due to the lack of a comprehensive understanding of the degradation mechanism of OSCs, further studies are needed to achieve effective material design strategies that enable simultaneously achieving a high PCE and a long device lifetime. Recent novel NFAs with fused-ring structures have led to rapid improvement in PCE; however, they still suffer from complexity in their synthetic routes. For instance, typically eight steps are required for synthesizing ITIC, an iconic NFA, from affordable commercially available materials,[34] and Y6 requires even more than 10 steps,[6] which leads to high material costs. Recently, non-fused-ring NFAs have attracted interest as cheaper alternatives to expensive fused-ring NFAs. PCE based on non-fused-ring NFAs has rapidly improved, and now exceeds 15%.[35] Further studies are needed to develop non-fused-ring NFAs that exhibit a high PCE comparable or even superior to those based on fused-ring NFAs with lower material costs.

Supporting Information

Supporting Information is available from the Wiley Online Library or from the author.

Acknowledgements

The author is grateful to Rei Shirouchi and Kazuki Kohzuki for their support in revising the manuscript. This study was partly supported by the JST PRESTO program Grant no. JPMJPR1874, and JSPS KAKENHI Grant nos. 17K14527, 21H02012, 21H05394, and 22K19065.

Conflict of Interest

The author declares no conflict of interest.

Keywords

fill factors, nonfullerene acceptors, open-circuit voltages, organic photovoltaics, power conversion efficiencies, short-circuit current densities

Received: October 1, 2022
Revised: October 31, 2022
Published online: November 11, 2022

[1] a) M. A. Green, *Prog. Photovoltaics* **2012**, *20*, 472; b) K. Yoshikawa, H. Kawasaki, W. Yoshida, T. Irie, K. Konishi, K. Nakano, T. Uto, D. Adachi, M. Kanematsu, H. Uzu, K. Yamamoto, *Nat. Energy* **2017**, *2*, 17032; c) M. A. Green, A. W. Y. Ho-Baillie, *ACS Energy Lett.* **2019**, *4*, 1639; d) M. A. Green, E. D. Dunlop, J. Hohl-Ebinger, M. Yoshita, N. Kopidakis, K. Bothe, D. Hinken, M. Rauer, X. Hao, *Prog. Photovoltaics* **2022**, *30*, 687; e) Y. Zhao, F. Ma, Z. Qu, S. Yu, T. Shen, H.-X. Deng, X. Chu, X. Peng, Y. Yuan, X. Zhang, J. You, *Science* **2022**, *377*, 531.

[2] a) Q. Liu, Y. Jiang, K. Jin, J. Qin, J. Xu, W. Li, J. Xiong, J. Liu, Z. Xiao, K. Sun, S. Yang, X. Zhang, L. Ding, *Sci. Bull.* **2020**, *65*, 272; b) P. Bi, S. Zhang, Z. Chen, Y. Xu, Y. Cui, T. Zhang, J. Ren, J. Qin, L. Hong, X. Hao, J. Hou, *Joule* **2021**, *5*, 2408; c) T. Zhang, C. An, P. Bi, Q. Lv, J. Qin, L. Hong, Y. Cui, S. Zhang, J. Hou, *Adv. Energy Mater.* **2021**, *11*, 2101705; d) Y. Cai, Y. Li, R. Wang, H. Wu, Z. Chen, J. Zhang, Z. Ma, X. Hao, Y. Zhao, C. Zhang, F. Huang, Y. Sun, *Adv. Mater.* **2021**, *33*, 2101733; e) Y. Cui, Y. Xu, H. Yao, P. Bi, L. Hong, J. Zhang, Y. Zu, T. Zhang, J. Qin, J. Ren, Z. Chen, C. He, X. Hao, Z. Wei, J. Hou, *Adv. Mater.* **2021**, *33*, 2102420; f) M. Zhang, L. Zhu, G. Zhou, T. Hao, C. Qiu, Z. Zhao, Q. Hu, B. W. Larson, H. Zhu, Z. Ma, Z. Tang, W. Feng, Y. Zhang, T. P. Russell, F. Liu, *Nat. Commun.* **2021**, *12*, 309; g) L. Zhan, S. Li, X. Xia, Y. Li, X. Lu, L. Zuo, M. Shi, H. Chen, *Adv. Mater.* **2021**, *33*, 2007231; h) Y. Wei, Z. Chen, G. Lu, N. Yu, C. Li, J. Gao, X. Gu, X. Hao, G. Lu, Z. Tang, J. Zhang, Z. Wei, X. Zhang, H. Huang, *Adv. Mater.* **2022**, *34*, 2204718; i) W. Gao, F. Qi, Z. Peng, F. R. Lin, K. Jiang, C. Zhong, W. Kaminsky, Z. Guan, C.-S. Lee, T. J. Marks, H. Ade, A. K.-Y. Jen, *Adv. Mater.* **2022**, *34*, 2202089; j) C. He, Y. Pan, Y. Ouyang, Q. Shen, Y. Gao, K. Yan, J. Fang, Y. Chen, C.-Q. Ma, J. Min, C. Zhang, L. Zuo, H. Chen, *Energy Environ. Sci.* **2022**, *15*, 2537; k) L. Zhan, S. Li, Y. Li, R. Sun, J. Min, Z. Bi, W. Ma, Z. Chen, G. Zhou, H. Zhu, M. Shi, L. Zuo, H. Chen, *Joule* **2022**, *6*, 662; l) L. Zhu, M. Zhang, J. Xu, C. Li, J. Yan, G. Zhou, W. Zhong, T. Hao, J. Song, X. Xue, Z. Zhou, R. Zeng, H. Zhu, C.-C. Chen, R. C. I. MacKenzie, Y. Zou, J. Nelson, Y. Zhang, Y. Sun, F. Liu, *Nat. Mater.* **2022**, *21*, 656; m) R. Sun, Y. Wu, X. Yang, Y. Gao, Z. Chen, K. Li, J. Qiao, T. Wang, J. Guo, C. Liu, X. Hao, H. Zhu, J. Min, *Adv. Mater.* **2022**, *34*, 2110147; n) J. Qin, Q. Yang, J. Oh, S. Chen, G. O. Odunmbaku, N. A. N. Ouedraogo, C. Yang, K. Sun, S. Lu, *Adv. Sci.* **2022**, *9*, 2105347; o) Y. Cai, Q. Li, G. Lu, H. S. Ryu, Y. Li, H. Jin, Z. Chen, Z. Tang, G. Lu, X. Hao, H. Y. Woo, C. Zhang, Y. Sun, *Nat. Commun.* **2022**, *13*, 2369.

[3] Z. Zheng, J. Wang, P. Bi, J. Ren, Y. Wang, Y. Yang, X. Liu, S. Zhang, J. Hou, *Joule* **2022**, *6*, 171.

[4] a) J. Hou, O. Inganäs, R. H. Friend, F. Gao, *Nat. Mater.* **2018**, *17*, 119; b) G. Y. Zhang, J. B. Zhao, P. C. Y. Chow, K. Jiang, J. Q. Zhang, Z. L. Zhu, J. Zhang, F. Huang, H. Yan, *Chem. Rev.* **2018**, *118*, 3447;

c) A. Wadsworth, M. Moser, A. Marks, M. S. Little, N. Gasparini, C. J. Brabec, D. Baran, I. McCulloch, *Chem. Soc. Rev.* **2019**, *48*, 1596; d) A. Armin, W. Li, O. J. Sandberg, Z. Xiao, L. Ding, J. Nelson, D. Neher, K. Vandewal, S. Shoaee, T. Wang, H. Ade, T. Heumüller, C. Brabec, P. Meredith, *Adv. Energy Mater.* **2021**, *11*, 2003570.

[5] a) J. Yuan, T. Huang, P. Cheng, Y. Zou, H. Zhang, J. L. Yang, S.-Y. Chang, Z. Zhang, W. Huang, R. Wang, D. Meng, F. Gao, Y. Yang, *Nat. Commun.* **2019**, *10*, 570; b) Y. Yang, *ACS Nano* **2021**, *15*, 18679.

[6] J. Yuan, Y. Q. Zhang, L. Y. Zhou, G. C. Zhang, H. L. Yip, T. K. Lau, X. H. Lu, C. Zhu, H. J. Peng, P. A. Johnson, M. Leclerc, Y. Cao, J. Ulanski, Y. F. Li, Y. P. Zou, *Joule* **2019**, *3*, 1140.

[7] a) H. Sahu, W. Rao, A. Troisi, H. Ma, *Adv. Energy Mater.* **2018**, *8*, 1801032; b) A. Mahmood, J.-L. Wang, *Energy Environ. Sci.* **2021**, *14*, 90; c) Y. Miyake, A. Saeki, *J. Phys. Chem. Lett.* **2021**, *12*, 12391.

[8] W. Shockley, H. J. Queisser, *J. Appl. Phys.* **1961**, *32*, 510.

[9] Y. Tamai, *Aggregate* **2022**, in press, https://doi.org/10.1002/agt2.280.

[10] S. Natsuda, T. Saito, R. Shirouchi, Y. Sakamoto, T. Takeyama, Y. Tamai, H. Ohkita, *Energy Environ. Sci.* **2022**, *15*, 1545.

[11] a) M. B. Smith, J. Michl, *Chem. Rev.* **2010**, *110*, 6891; b) Y. Tamai, H. Ohkita, H. Benten, S. Ito, *J. Phys. Chem. C* **2013**, *117*, 10277; c) Y. Kasai, Y. Tamai, H. Ohkita, H. Benten, S. Ito, *J. Am. Chem. Soc.* **2015**, *137*, 15980.

[12] a) T. N. Singh-Rachford, F. N. Castellano, *Coord. Chem. Rev.* **2010**, *254*, 2560; b) Y. Tamai, H. Ohkita, H. Benten, S. Ito, *Chem. Mater.* **2014**, *26*, 2733; c) B. Joarder, N. Yanai, N. Kimizuka, *J. Phys. Chem. Lett.* **2018**, *9*, 4613; d) Y. Sakamoto, Y. Tamai, H. Ohkita, *J. Chem. Phys.* **2020**, *153*, 161102.

[13] a) S. Izawa, M. Hiramoto, *Nat. Photonics* **2021**, *15*, 895; b) Y. Sakamoto, S. Izawa, H. Ohkita, M. Hiramoto, Y. Tamai, *Commun. Mater.* **2022**, *3*, 76.

[14] a) U. Rau, *Phys. Rev. B* **2007**, *76*, 085303; b) J. Yao, T. Kirchartz, M. S. Vezie, M. A. Faist, W. Gong, Z. He, H. Wu, J. Troughton, T. Watson, D. Bryant, J. Nelson, *Phys. Rev. Appl.* **2015**, *4*, 014020.

[15] T. Saito, S. Natsuda, K. Imakita, Y. Tamai, H. Ohkita, *Sol. RRL* **2020**, *4*, 2000255.

[16] J. Benduhn, K. Tvingstedt, F. Piersimoni, S. Ullbrich, Y. Fan, M. Tropiano, K. A. McGarry, O. Zeika, M. K. Riede, C. J. Douglas, S. Barlow, S. R. Marder, D. Neher, D. Spoltore, K. Vandewal, *Nat. Energy* **2017**, *2*, 17053.

[17] a) F. D. Eisner, M. Azzouzi, Z. Fei, X. Hou, T. D. Anthopoulos, T. J. S. Dennis, M. Heeney, J. Nelson, *J. Am. Chem. Soc.* **2019**, *141*, 6362; b) G. Han, Y. Yi, *J. Phys. Chem. Lett.* **2019**, *10*, 2911; c) X.-K. Chen, D. Qian, Y. Wang, T. Kirchartz, W. Tress, H. Yao, J. Yuan, M. Hülsbeck, M. Zhang, Y. Zou, Y. Sun, Y. Li, J. Hou, O. Inganäs, V. Coropceanu, J.-L. Bredas, F. Gao, *Nat. Energy* **2021**, *6*, 799.

[18] S. Natsuda, T. Saito, R. Shirouchi, K. Imakita, Y. Tamai, *Polym. J.* **2022**, *54*, 1345.

[19] a) H. Uoyama, K. Goushi, K. Shizu, H. Nomura, C. Adachi, *Nature* **2012**, *492*, 234; b) H. Nakanotani, Y. Tsuchiya, C. Adachi, *Chem. Lett.* **2021**, *50*, 938.

[20] a) D. Veldman, Ö. İpek, S. C. J. Meskers, J. Sweelssen, M. M. Koetse, S. C. Veenstra, J. M. Kroon, S. S. van Bavel, J. Loos, R. A. J. Janssen, *J. Am. Chem. Soc.* **2008**, *130*, 7721; b) S. H. Park, A. Roy, S. Beaupré, S. Cho, N. Coates, J. S. Moon, D. Moses, M. Leclerc, K. Lee, A. J. Heeger, *Nat. Photonics* **2009**, *3*, 297; c) S. Shoaee, M. P. Eng, E. Espíldora, J. L. Delgado, B. Campo, N. Martín, D. Vanderzande, J. R. Durrant, *Energy Environ. Sci.* **2010**, *3*, 971; d) F. Etzold, I. A. Howard, N. Forler, D. M. Cho, M. Meister, H. Mangold, J. Shu, M. R. Hansen, K. Mullen, F. Laquai, *J. Am. Chem. Soc.* **2012**, *134*, 10569; e) S. Shoaee, S. Subramaniyan, H. Xin, C. Keiderling, P. S. Tuladhar, F. Jamieson, S. A. Jenekhe, J. R. Durrant, *Adv. Funct. Mater.* **2013**, *23*, 3286; f) Y. Tamai, K. Tsuda, H. Ohkita, H. Benten, S. Ito, *Phys. Chem. Chem. Phys.* **2014**, *16*, 20338; g) A. C. Jakowetz, M. L. Böhm, J. Zhang, A. Sadhanala, S. Huettner, A. A. Bakulin, A. Rao, R. H. Friend, *J. Am. Chem. Soc.* **2016**, *138*, 11672; h) Y. Tamai, Y. Fan, V. O. Kim, K. Ziabrev, A. Rao, S. Barlow, S. R. Marder, R. H. Friend, S. M. Menke, *ACS Nano* **2017**, *11*, 12473; i) Y. Tamai, *Polym. J.* **2020**, *52*, 691; j) S. Natsuda, T. Saito, R. Shirouchi, K. Imakita, Y. Tamai, *Polym. J.* **2022**, *54*, 1345.

[21] S. M. Menke, A. Cheminal, P. Conaghan, N. A. Ran, N. C. Greehnam, G. C. Bazan, T. Q. Nguyen, A. Rao, R. H. Friend, *Nat. Commun.* **2018**, *9*, 277.

[22] A. J. Gillett, A. Privitera, R. Dilmurat, A. Karki, D. Qian, A. Pershin, G. Londi, W. K. Myers, J. Lee, J. Yuan, S.-J. Ko, M. K. Riede, F. Gao, G. C. Bazan, A. Rao, T.-Q. Nguyen, D. Beljonne, R. H. Friend, *Nature* **2021**, *597*, 666.

[23] S. Natsuda, Y. Sakamoto, T. Takeyama, R. Shirouchi, T. Saito, Y. Tamai, H. Ohkita, *J. Phys. Chem. C* **2021**, *125*, 20806.

[24] R. A. Marcus, *Rev. Mod. Phys.* **1993**, *65*, 599.

[25] N. Aizawa, Y.-J. Pu, Y. Harabuchi, A. Nihonyanagi, R. Ibuka, H. Inuzuka, B. Dhara, Y. Koyama, K.-I. Nakayama, S. Maeda, F. Araoka, D. Miyajima, *Nature* **2022**, *609*, 502.

[26] M. A. Green, *Solid-State Electron.* **1981**, *24*, 788.

[27] a) G. Yu, J. Gao, J. C. Hummelen, F. Wudl, A. J. Heeger, *Science* **1995**, *270*, 1789; b) J. J. M. Halls, C. A. Walsh, N. C. Greenham, E. A. Marseglia, R. H. Friend, S. C. Moratti, A. B. Holmes, *Nature* **1995**, *376*, 498.

[28] Y. Tamai, H. Ohkita, H. Benten, S. Ito, *J. Phys. Chem. Lett.* **2015**, *6*, 3417.

[29] a) T. Umeyama, K. Igarashi, D. Sasada, Y. Tamai, K. Ishida, T. Koganezawa, S. Ohtani, K. Tanaka, H. Ohkita, H. Imahori, *Chem. Sci.* **2020**, *11*, 3250; b) T. Umeyama, K. Igarashi, Y. Tamai, T. Wada, T. Takeyama, D. Sasada, K. Ishida, T. Koganezawa, S. Ohtani, K. Tanaka, H. Ohkita, H. Imahori, *Sustainable Energy Fuels* **2021**, *5*, 2028.

[30] A. J. Sneyd, T. Fukui, D. Paleček, S. Prodhan, I. Wagner, Y. Zhang, J. Sung, S. M. Collins, T. J. A. Slater, Z. Andaji-Garmaroudi, L. R. MacFarlane, J. D. Garcia-Hernandez, L. Wang, G. R. Whittell, J. M. Hodgkiss, K. Chen, D. Beljonne, I. Manners, R. H. Friend, A. Rao, *Sci. Adv.* **2021**, *7*, eabh4232.

[31] a) H. Liu, Y. Li, S. Xu, Y. Zhou, Z. A. Li, *Adv. Funct. Mater.* **2021**, *31*, 2106735; b) H. Liu, M.-H. Yu, C.-C. Lee, X. Yu, Y. Li, Z. Zhu, C.-C. Chueh, Z. A. Li, A. K.-Y. Jen, *Adv. Mater. Technol.* **2021**, *6*, 2000960; c) Y. Li, J. Yu, Y. Zhou, Z. A. Li, *Chem. Eur. J.* **2022**, *28*, e202201675.

[32] R. Sun, W. Wang, H. Yu, Z. Chen, X. Xia, H. Shen, J. Guo, M. Shi, Y. Zheng, Y. Wu, W. Yang, T. Wang, Q. Wu, Y. Yang, X. Lu, J. Xia, C. J. Brabec, H. Yan, Y. Li, J. Min, *Joule* **2021**, *5*, 1548.

[33] X. Du, T. Heumueller, W. Gruber, A. Classen, T. Unruh, N. Li, C. J. Brabec, *Joule* **2019**, *3*, 215.

[34] Y. Lin, J. Wang, Z.-G. Zhang, H. Bai, Y. Li, D. Zhu, X. Zhan, *Adv. Mater.* **2015**, *27*, 1170.

[35] L. Ma, S. Zhang, J. Zhu, J. Wang, J. Ren, J. Zhang, J. Hou, *Nat. Commun.* **2021**, *12*, 5093.

Yasunari Tamai received his Ph.D. degree from Kyoto University in 2013 on the excited-state dynamics in nanostructured polymer systems. He joined the optoelectronics group at the University of Cambridge as a postdoctoral fellow under the supervision of Prof. Sir Richard Friend, where his research focused on the ultrafast charge separation at organic semiconductor heterojunctions. Since 2016, he has been an assistant professor at Kyoto University. From 2018 to 2022, he was also a JST PRESTO researcher. His current research interests include exciton and charge dynamics in organic semiconductors, particularly conjugated polymers.